



First experimental identification of Ras-inhibitor binding interface using a water-soluble Ras ligand

Alessandro Palmioli^a, Elena Sacco^a, Sherwin Abraham^c, Celestine J. Thomas^b, Alessandro Di Domizio^a, Luca De Gioia^a, Vadim Gaponenko^c, Marco Vanoni^a, Francesco Peri^{a,*}

^a Department of Biotechnology and Biosciences, University of Milano-Bicocca, Piazza della Scienza, 2, 20126 Milano, Italy

^b Center for Biomolecular Structure and Dynamics (CBSD), Chem-218, 32 Campus Dr, University of Montana, Missoula, MT 59812, United States

^c Department of Biochemistry and Molecular Genetics University of Illinois at Chicago, 900 S. Ashland Ave. Chicago, IL 60607, United States

ARTICLE INFO

Article history:

Received 10 March 2009

Revised 26 May 2009

Accepted 27 May 2009

Available online 30 May 2009

Keywords:

Ras protein

Sugars

Synthesis

Anticancer agents

NMR

Molecular modeling

ABSTRACT

By combining in the same molecule Ras-interacting aromatic moieties and a sugar, we prepared a water-soluble Ras ligand that binds Ras and inhibits guanine nucleotide exchange. With this compound it was possible to determine experimentally by a ¹⁵N-edited HSQC NMR experiment the ligand-Ras binding interface.

© 2009 Elsevier Ltd. All rights reserved.

Ras, a key member in the super-family of small GTPases, is an essential component of signal transduction pathways that regulate cell growth, proliferation, differentiation and apoptosis.^{1–3} Operating as molecular switches, Ras GTPases, assisted by guanine exchange factors (GEFs), undergo nucleotide exchange, allowing them to rapidly cycle from the inactive GDP⁴ bound state to the activated GTP bound state. The active Ras, aided by GTPase activating proteins (GAPs), hydrolyses the bound GTP to GDP and returns to the inactive GDP bound state.^{5,6} Alteration of this deactivating reaction is a common biochemical defect associated with oncogenic Ras mutants.^{7–9} Oncogenic Ras mutants exhibit decreased hydrolytic efficiency due to reduced affinities towards GAP proteins.¹⁰

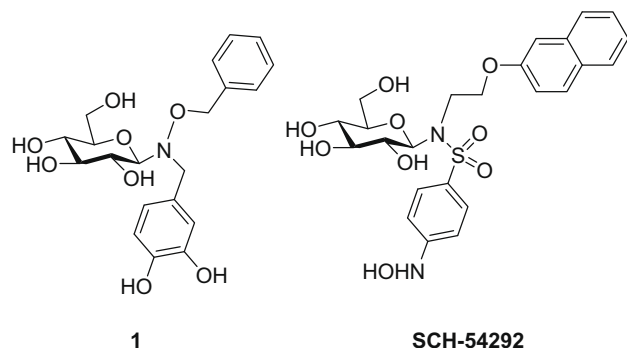
Identifying small drug molecules that selectively interact with oncogenic Ras proteins and inhibit constitutive Ras activation is a challenging and a still largely unsolved task. The prolonged lifetimes of activated oncogenic Ras mutants can, in principle, be reduced by the action of drugs that are capable of converting the oncogenic states to behave like normal phenotypes. This can be achieved by molecules that either inhibit the process of GEF-catalyzed GTP loading on inactive Ras-GDP^{11,12} or by simply accelerating the GTP hydrolysis in the active Ras-GTP complex.^{13–15} While

several efforts have been made in developing agents that accelerate the rate of GTP hydrolysis (self-hydrolyzing GTP analogues), very limited strategies directed at inhibiting GEF-catalyzed nucleotide exchange have been undertaken. To address this issue, our group has been actively engaged in developing sugar-derived ligands that can inhibit GEF-promoted guanine nucleotide exchange on H-Ras. Several generations of compounds, composed of a sugar moiety or a linear spacer to which aromatic pharmacophore groups are covalently linked, were synthesized and evaluated for Ras inhibitory activity.^{16–20} These small organic molecules (whose MW ranges from 300 to 500 Da) bind to H-Ras-GDP with micromolar affinity and inhibit GEF-Ras interaction thereby preventing guanine nucleotide exchange. All of these inhibitors seem to recognize a common binding site on Ras. In silico docking studies indicated that amino acid residues Y96, G60, Q61 and E62 of H-Ras exhibit strong interactions with these inhibitors. Hence a binding interface that partially overlaps with the Switch II region (residues 60–76) was identified to be a plausible binding pocket.^{17,18} Our earlier experiments using Surface Plasmon Resonance (SPR) studies indicated that arabinose and glucose-derived compounds interfere with the interaction of GEF molecules with H-Ras, reinforcing our hypothesis that these inhibitors bind to a site proximal to the Switch II region.²⁰ However, the exact mode of action of these nucleotide exchange inhibitors is currently unknown since no structure of an inhibitor bound Ras-GDP

* Corresponding author.

E-mail address: francesco.peri@unimib.it (F. Peri).

complex is available. The low aqueous solubility of these compounds hampered meaningful NMR and crystallography studies and therefore most insights were derived only from computational analysis. Indeed numerous efforts by our group to co-crystallize the hydroxylamine-containing inhibitors with Ras were unsuccessful.²¹ The extremely low water solubility of these compounds necessitated the addition of at least 10% methanol that resulted in aggregation and precipitation of H-Ras, leading to a generalized shift of cross-peaks in 2D NMR spectra.



Structures of compounds **SCH-54292** and **1**.

In this Letter we present the first experimental characterization of the H-Ras binding site using a rationally designed water-soluble H-Ras ligand. The design of compound **1** was inspired by the N-glycosylated sulphonamide **SCH-54292** previously synthesized by Schering Plough laboratories and used in NMR experiments to evaluate binding to H-Ras.¹² We re-synthesized compound **SCH-54292** and found it to be almost completely insoluble at the concentrations required for NMR-based binding experiments. Compound **1** was tailored specifically to overcome this insolubility issue associated with previously developed H-Ras inhibitors. Our molecule is composed of an O-Benzyl-N-(3,4-dihydroxybenzyl) hydroxylamine moiety that is N-glycosylated with D-glucose. To ensure water-solubility, the hydrophylic sugar and dihydroxybenzyl moieties were included in the design of **1**, and the hydrophobic naphthyl of **SCH-54292** was replaced with a benzyl group. The key step in the synthesis of **1** is the chemoselective glucosylation of the O-benzyl-N-(3,4-dihydroxybenzyl) hydroxylamine **3** (Scheme 1).

Our group pioneered the chemoselective formation of glycosidic bonds between reducing sugars and a N,O-disubstituted hydroxylamines to form 'neoglycosides' and this method is now extensively used by other research groups for the preparation of libraries of differently glycosylated bioactive compounds ranging from neoglycopeptides, neooligosaccharides to neoglycosteroids and antibiotics.^{22–27} The notable advantage that this approach

provides, over traditional chemical glycosylation reactions, is the use of unprotected and non-activated reducing sugar moieties as glycosyl donors. Additionally, the final neoglycoside product is obtained stereoselectively (at least in the case of glucose, galactose and glucosamine-N-acetyl) in the β -anomeric configuration. This highly convergent and efficient synthetic strategy can be effectively employed for the preparation of an array of potential Ras ligands, in which different reducing mono- or oligosaccharides are combined with N,O-disubstituted hydroxylamines through a β -N glycosidic linkage.

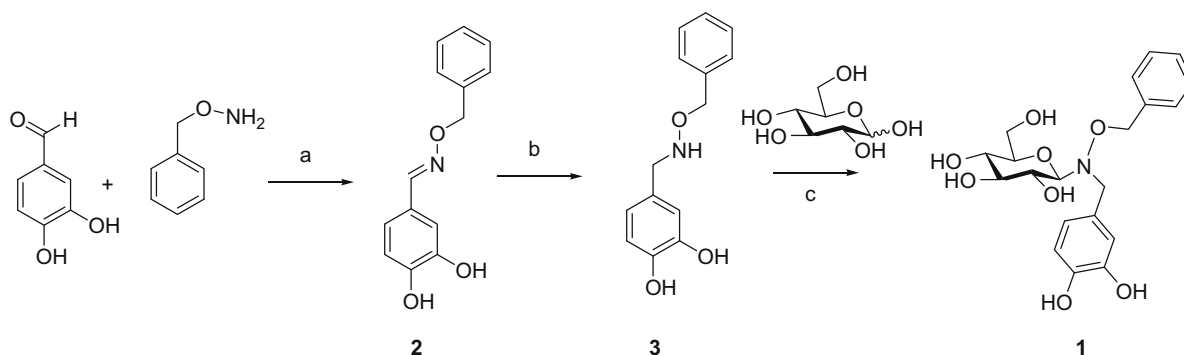
For the synthesis of compound **1**, commercially available 3,4-dihydroxybenzaldehyde was reacted with O-benzylhydroxylamine hydrochloride in pyridine at rt, 12 h, affording the corresponding O-benzyl oxime **2** with 98% yield. The oxime was reduced to the 4-[(benzyloxyamino)methyl]benzene-1,2-diol **3** by treatment with NaCNBH₃ in acetic acid at r.t. for 2 h (80% yield). The hydroxylamine **3** and D-glucose were then reacted in DMF/AcOH/aqueous acetate buffer pH 4.5 (1:1:1) at 50 °C overnight affording compound **1** in 80% yield.

In contrast to all Ras inhibitors (including **SCH-54292**) synthesized and tested by our group, compound **1** was clearly soluble in water or TRIS buffers to a concentration of several mM, and was stable at neutral pH for months (as assessed by TLC and HPLC analyses).

Isothermal titration calorimetric (ITC) studies were performed to quantify the affinity of compound **1** towards H-Ras (1–166). This molecule was able to bind to H-Ras with an affinity of 37 μ M and with an enthalpy of binding of -1964 ± 40 cal/mol (error was calculated on the basis of three independent titrations).

Compound **1** exhibited exothermic heats in ITC profile. Interestingly the stoichiometric value of the compound **1**: H-Ras interaction was 1:1 (equimolar). Figure 1S (Supplementary data) indicates the binding to H-Ras to compound **1**.

Compound **1** was then tested for its ability to bind H-Ras-GDP (1–166) by NMR experiments in solution. The titration of compound **1** into a solution of ¹⁵N H-Ras (1–166) was followed by ¹⁵N-edited HSQC experiments that allowed delineation of the Ras–ligand binding interface. A series of spectra was collected at different Ras:ligand molar ratios. The results of these experiments are depicted in Figure 1. The residues exhibiting statistically significant chemical shift perturbations are marked on the graph. Upon titration with **1**, several cross-peak chemical shifts changed, while most signals did not show significant perturbations (Fig. 1A). The changes in chemical shifts were concentration-dependent as shown in Figure 1B–D. The presence of fast exchange on the NMR time-scale evident in Figure 1B–D is in agreement with low micromolar binding affinity of **1** for H-Ras-GDP as observed in ITC studies. The statistically significant chemical shift perturbations were observed in the β -3 strand (residues I55, T58, A59, and Y64) of the central β -sheet and α -2 helix (residues M67, R68,



Scheme 1. Chemoselective synthesis of compound **1**. Reagents and conditions: (a) dry pyridine, 98%; (b) NaCNBH₃, glacial AcOH, 80%; (c) DMF/AcOH/aqueous acetate buffer at pH 4.5, 80%.

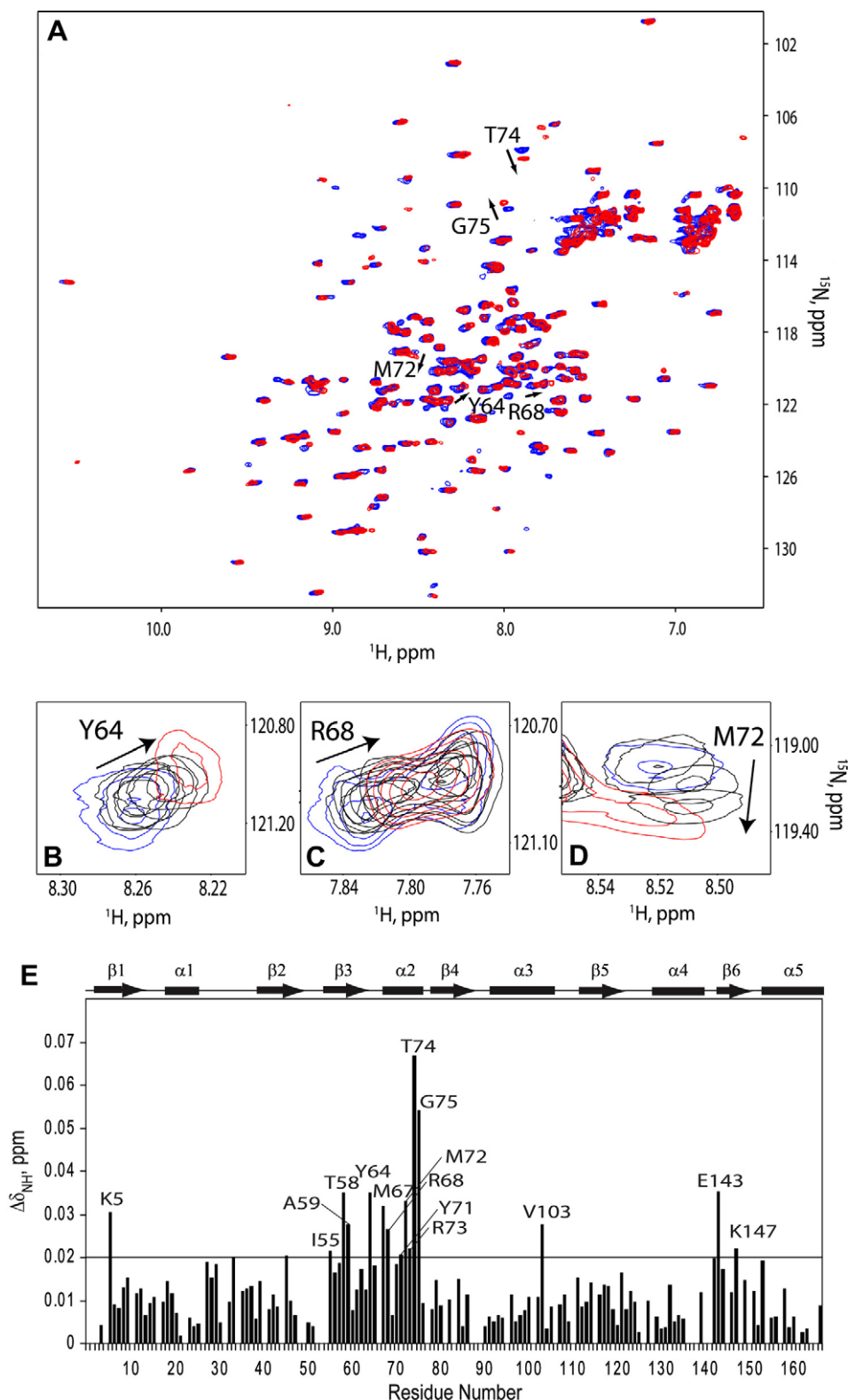


Figure 1. NMR titration of H-Ras-GDP 1–166 with compound **1**. (A) ^{15}N HSQC spectra of H-Ras-GDP 1–166 with 0 (blue) and 20 M equiv of compound **1** (red) are superimposed. Examples of chemical shift perturbations are marked. Spectral inserts for Y64 (B), R68 (C), and M72 (D) show addition of 0 (blue), 1, 2, 5, 10, and 20 (red) M equiv of compound **1**. The arrows mark the direction of chemical shift changes. (E) normalized HN chemical shift perturbations. The boxes and arrows above the graph represent helices and sheets in H-Ras-GDP 1–166.²⁸ The horizontal line marks the average value of chemical shift perturbations plus one standard deviation.

Y71, M72, R73, T74 and G75) as shown in Figure 1E. Residues K5 and V103 are adjacent to the β -3/ α -2 region and complete a

continuous binding site of the drug lead compound on the catalytic domain of H-Ras-GDP.

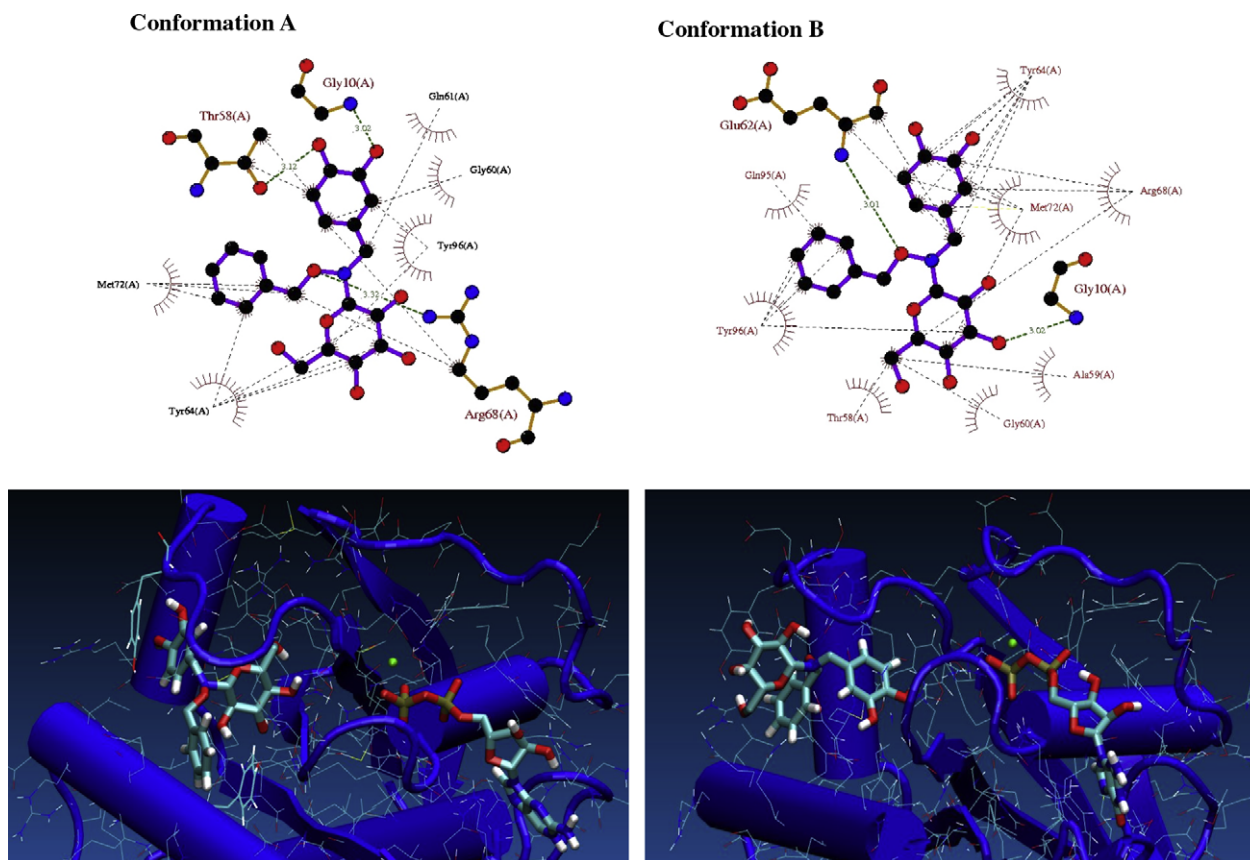


Figure 2. (A) Contact maps and (B) 3D representations of the two most representative lowest-energy protein–ligand complexes (termed as A and B) as obtained from MD calculations starting from the best docking results of compound **1**.

The crosspeak shifts observed in HSQC experiments are caused by a variation in the electromagnetic environment of the amino acids. This may indicate direct binding with ligand or structural rearrangement of the protein due to binding. In the case of residues E143 and K147 that do not belong to the continuous binding site, the chemical shift variations outlined in Figure 1E may be due to a remote or propagated structural change of Ras induced by ligand binding.

The NMR binding data were complemented by molecular dynamic (MD) and docking experiments. Assuming the cleft in the vicinity of the Switch II region of H-Ras as the receptor binding site, we docked compound **1** into the rigid structure of human H-Ras derived from crystallographic coordinates (PDB code: 4q21). Two principal clusters of ligand arrangements were obtained and docking energies of the two lowest energy protein–ligand complexes are -6.41 and -5.91 kcal/mol, respectively (Fig. 2).

Explicit solvent MD simulations were then carried out starting from the best protein–ligand complexes obtained by docking calculations, with the aim of refining and improving docking results including solvent effects and accounting for induced fit.²⁹ The MD refined structures, obtained starting from cluster A and B geometries, were then analyzed, with the aim of highlighting protein residues for which different chemical shifts are expected to deviate from the unbound (H-Ras-GDP) to the bound (H-Ras-GDP-**1**) structures. In particular, protein residues which drastically change their chemical environment are listed in Table 1S (Supplementary data).

In order to correlate binding data with biochemical activity, the inhibitory effect of compound **1** on the GEF-catalyzed exchange of H-Ras-bound GDP was tested. The catalytic domain of Ras-specific GEF RasGRF1 was used to promote exchange as described earlier.³⁰

Exchange assays were performed in the presence of increasing concentrations of compound **1** (0, 50, 100, 250 and 500 μM) (Fig. 3A). The initial rate of each exchange reaction, calculated as described in Supplementary data was plotted as a function of compound concentration (dose–response curve, Fig. 3B). It is evident that at 100 μM compound **1** induce about a fifty percent of inhibition of the GEF-catalyzed exchange rate on H-Ras. Circular Dichroism experiments (data not shown) demonstrated that binding of compound **1** to Ras does not induce protein denaturation nor damages the protein structure.

To verify the activity of **1** on cells, experiments that monitor the rate of proliferation were performed using NIH3T3 mouse fibroblasts. Cells were plated at a density of 3000 cells/cm² and left to adhere onto plastic surface for 18 h. Then cells were treated with **1** (at concentrations 0, 50, 150 and 450 μM) supplemented in the growth medium, and counted at 24, 48 and 72 h after treatment. The obtained growth curves (Fig. 4A) and morphological analysis of treated cells (Fig. 4B) demonstrate that compound **1** at 150 μM effectively inhibits cell proliferation. In fact the number of cells treated with 150 μM and 450 μM **1** at 24 h from treatment is lower than control and does not increase later in time. Accordingly, in the culture medium of treated cells (Panel B) it is possible to appreciate many dead cells in suspension (refrangent cells circled in white).^{31,32}

The data presented here point out that compound **1** binds to H-Ras with low affinity but it is capable of inhibiting GEF-mediated nucleotide exchange. The ITC experiments conclude that compound **1** has a μM affinity towards H-Ras-GDP and that 1:1 Ras–ligand complex is formed.

NMR and MD based experimental results converge to indicate that certain H-Ras residues are critical for ligand binding. These in-

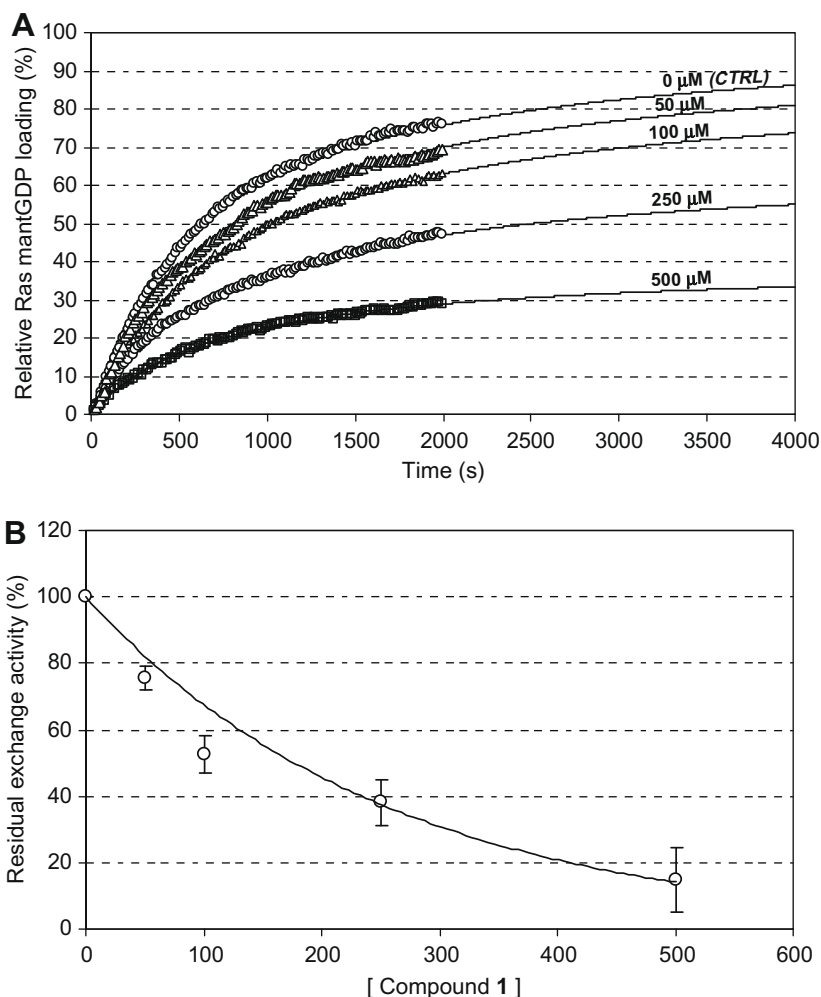


Figure 3. Effect of compound **1** on GEF-catalyzed nucleotide exchange of H-Ras. (A) Stimulation of the GDP to mantGDP exchange reaction on H-Ras determined adding to 0.25 μM H-Ras-GDP, 1.25 mM mantGDP, 0.0625 μM RasGRF1 and different concentrations (0, 50, 100, 250 and 500 μM) of compound **1**. Fluorescence measurements were made with a Perkin–Elmer LS-45 luminescence spectrometer, monitoring the fluorescence each second for at least 1500 sec. For graphical reason in figure only a point every 15 has been plotted. Each experimental curve was fitted to a non linear ‘growth-sigmoidal Hill’ curve ($n = 1$) with OriginPro 8.0 software, reported in graph as a thin line. In the graph the maximum value of relative fluorescence (100 on Y-axis) represent the fully charged Ras status obtained as plateau of an exchange curve without compound. For each reaction the initial exchange rate was calculated as first derivative at time 0 with OriginPro 8.0 software. (B) Dose–response curves of compound **1** on GEF-catalyzed exchange of Ras. The initial exchange rate of each exchange reaction (mean of at least three independent experiments) was plotted as a function of the compound concentration (dose–response curves). The exchange rate of control reaction (performed without compound) was normalized to 100.

clude amino acids T58, A59 and Y64 belonging to the β -3 strand and R68, M72 on the α -2 helix. The observed binding site covers a region that is essential for Ras interactions with the Ras–GEF domain of RasGRF1, homologous to SOS, as described by the crystal structure of the Ras–SOS complex.³³ Therefore, it is possible that compound **1** interferes with H-Ras–GEF interaction, as previously outlined using SPR experiments.²⁰ The affinity of binding to H-Ras as calculated by ITC experiments (Fig. 1S) is in the same order of magnitude of the affinity between Ras–GDP and GEF.³⁴ This means that compound **1**, although having low affinity for Ras, can compete effectively with GEF for Ras binding thus inhibiting Ras activation.

In conclusion, because of the favorable solubility of the designed ligand, we were able to determine experimentally the Ras-inhibitor binding site as well as fundamental thermodynamic binding parameters. The involvement of sections of the Switch II region in inhibitor binding was previously hypothesized by us on the base of NMR STD experiments and is now conclusively demonstrated in this report. We are currently investigating whether global or allosteric conformational changes can occur upon

inhibitor binding to H-Ras, and how these may affect Ras-modulated downstream signaling events.

We consider the development of soluble inhibitors against mutant Ras super-family of GTPases as one of the strongest routes to provide clinically effective cancer therapeutics. We propose that our design and evaluation of small molecule inhibitors, such as compound **1**, may serve as templates on which future pharmacologically relevant drug design studies can be attempted.

Acknowledgements

The authors wish to thank Annalisa D'urzo for technical assistance. Dr. C. J. Thomas would like to thank Dr. Stephen R Sprang (SRS), Director of CBSD, University of Montana for his support in both space and instruments towards this project and also for the salary support from National Institutes of Health Grants DK46371. Dr. V. Gaponenko acknowledges the generous support from the American Cancer Society Grant RGS-09-057-01-GMC. Professor M. Vanoni acknowledges Creabilis and MIUR-FAR for financial support.

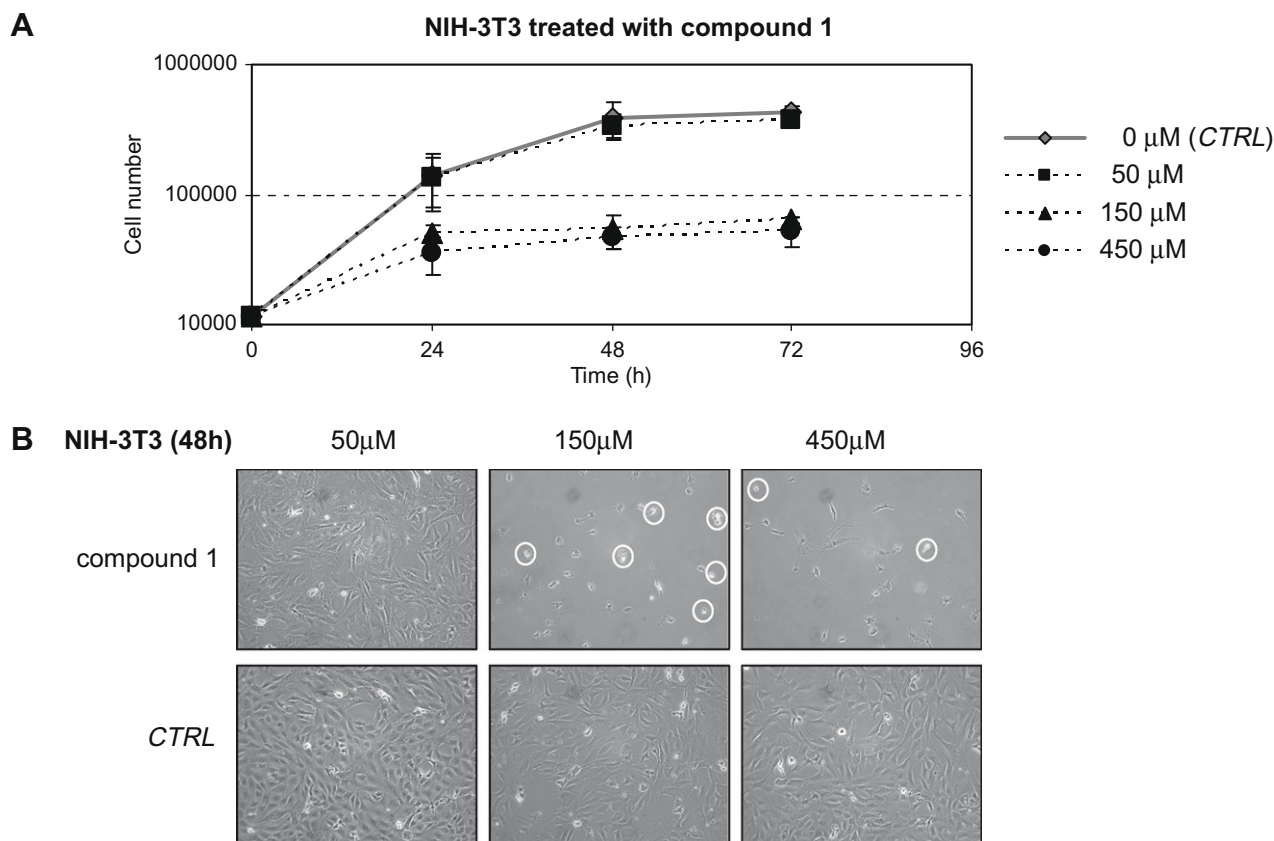


Figure 4. (A) Proliferation curves of NIH3T3 fibroblasts grown in media supplemented with different concentrations of compound **1**: 0 μM (grey diamond; CTRL = control), 50 μM (black square), 150 μM (black triangle) and 450 μM (black circle). Cells were counted after 24, 48 and 72 h of treatment with compound **1**. Plotted data are mean \pm s.d. computed from at least three independent experiments. (B) Morphological analysis of cells treated for 48 h with different concentrations of compound **1** (or buffer, CTRL). White circles indicate floating dead cells detached from the plate.

Supplementary data

Synthetic procedures, products characterization, biochemistry experiments, ITC experiments, NMR experiments, cell biology. Supplementary data associated with this article can be found in the online version, at doi:10.1016/j.bmcl.2009.05.107.

References and notes

- Barbacid, M. *Annu. Rev. Biochem.* **1987**, *56*, 779.
- Lowy, D. R.; Willumsen, B. M. *Annu. Rev. Biochem.* **1993**, *62*, 851.
- Vojtcek, A. B.; Der, C. J. *J. Biol. Chem.* **1998**, *273*, 19925.
- Abbreviations*: GDP, guanosine diphosphate; GTP, guanosine triphosphate; HPLC, high pressure chromatography; HSQC, heteronuclear single quantum coherence; STD, saturation transfer difference; TLC, thin layer chromatography.
- McCormick, F. *Cell* **1989**, *56*, 5.
- Bourne, H. R.; Sanders, D. A.; McCormick, F. *Nature* **1989**, *341*, 209.
- Waldmann, H.; Wittinghofer, A. *Angew. Chem., Int. Ed.* **2000**, *39*, 4192.
- Downward, J. *Nat. Rev. Cancer* **2002**, *3*, 11.
- Bos, J. L.; Rehmann, H.; Wittinghofer, A. *Cell* **2007**, *129*, 865.
- Buhrman, G.; Wink, G.; Mattos, C. *Structure* **2007**, *15*, 1618.
- Taveras, A. G.; Remiszewski, S. W.; Doll, R. J.; Cesarz, D.; Huang, E. C.; Kirschmeier, P.; Pramanik, B. N.; Snow, M. E.; Wang, Y.-S.; del Rosario, J. D.; Vibulbhan, B.; Bauer, B. B.; Brown, J. E.; Carr, D.; Catino, J.; Evans, C. A.; Girijavallabhan, V.; Heimark, L.; James, L.; Liberles, S.; Nash, C.; Perkins, L.; Senior, M. M.; Tzarbopoulos, A.; Ganguly, A. K.; Aust, R.; Brown, E.; Delisle, D.; Fuhrman, S.; Hendrickson, T.; Kissinger, C.; Love, R.; Sisson, W.; Villafranca, E.; Webber, S. E. *Bioorg. Med. Chem.* **1997**, *5*, 125.
- Ganguly, A. K.; Wang, Y.-S.; Pramanik, B. N.; Doll, R. J.; Snow, M. E.; Taveras, A. G.; Remiszewski, S.; Cesarz, D.; del Rosario, J.; Vibulbhan, B.; Brown, J. E.; Kirschmeier, P.; Huang, E. C.; Heimark, L.; Tzarbopoulos, A.; Girijavallabhan, V. M. *Biochemistry* **1998**, *37*, 15631.
- Zor, T.; Baryaacov, M.; Elgavish, S.; Shaanan, B.; Selinger, Z. *Eur. J. Biochem.* **1997**, *249*, 330.
- Zor, T.; Andorn, R.; Siofer, I.; Chorev, M.; Selinger, Z. *FEBS Lett.* **1998**, *433*, 326.
- Ahmadian, M. R.; Zor, T.; Kabsch, W.; Selinger, Z.; Wittinghofer, A.; Scheffzek, K. *Proc. Natl. Acad. Sci. U.S.A.* **1999**, *96*, 7065.
- Colombo, S.; Peri, F.; Tisi, R.; Nicotra, F.; Martegani, E. *Ann. NY Acad. Sci.* **2004**, *1030*, 52.
- Peri, F.; Airoidi, C.; Colombo, S.; Martegani, E.; van Neuren, A. S.; Stein, M.; Maranzi, C.; Nicotra, F. *ChemBioChem* **2005**, *6*, 1839.
- Peri, F.; Airoidi, C.; Colombo, S.; Mari, S.; Jiménez-Barbero, J.; Martegani, E.; Nicotra, F. *Eur. J. Org. Chem.* **2006**, 3707.
- Mueller, C.; Gomez-Zurita Frau, M. A.; Ballinari, D.; Colombo, S.; Bitto, A.; Martegani, E.; Airoidi, C.; van Neuren, A. S.; Stein, M.; Weiser, J.; Battistini, C.; Peri, F. *ChemMedChem* **2009**, *4*, 524.
- Airoidi, C.; Palmioli, A.; D'Urzo, A.; Colombo, S.; Vanoni, M.; Martegani, E.; Peri, F. *ChemBioChem* **2007**, 1376.
- H-Ras (1–166) bound to compound **1** was purified and subjected to crystallization trials. Many commercially available sparse matrix conditions were tried to identify crystallizing conditions, but currently have not resulted in hit. Preformed H-Ras crystals were soaked in crystallizing mother liquor containing excess dissolved compound **1** and were found to dissolve and not reappear even after prolonged storage.
- Peri, F.; Dumy, P.; Mutter, M. *Tetrahedron* **1998**, *54*, 12269.
- Peri, F.; Deutman, A.; La Ferla, B.; Nicotra, F. *Chem. Commun.* **2002**, 1504.
- Peri, F.; Nicotra, F. *Chem. Commun.* **2004**, 6, 623, and references therein.
- Langenhan, J. M.; Peters, N. R.; Guzei, I. A.; Hoffmann, F. M.; Thorson, J. S. *Proc. Natl. Acad. U.S.A.* **2005**, *102*, 12305.
- Ahmed, A.; Peters, N. R.; Fitzgerald, M. K.; Watson, J. A., Jr.; Hoffmann, F. M.; Thorson, J. S. *J. Am. Chem. Soc.* **2006**, *128*, 14224.
- Griffith, B. R.; Krepel, C.; Fu, X.; Blanchard, S.; Ahmed, A.; Edmiston, C. E.; Thorson, J. S. *J. Am. Chem. Soc.* **2007**, *129*, 8150.
- Kraulis, P. J.; Domaille, P. J.; Campbell-Burk, S. L.; Van Aken, T.; Laue, E. D. *Biochemistry* **1994**, *33*, 3515.
- Herna, A.; Andrei, A.; Bliznyuk, A.; Greedy, E. *Med. Res. Rev.* **2006**, *26*, 531.
- Lenzen, C.; Cool, R. H.; Wittinghofer, A. *Met. Enzymol.* **1995**, 255, 95.
- Chiaradonna, F.; Sacco, E.; Manzoni, R.; Giorgio, M.; Vanoni, M.; Alberghina, L. *Oncogene* **2006**, *25*, 5391.
- Gaglio, D.; Soldati, C.; Vanoni, M.; Alberghina, L.; Chiaradonna, F. *PLoS ONE* **2009**, *4*, e4715.
- Boriack-Sjodin, P. A.; Margarit, S. M.; Bar-Sagi, D.; Kuriyan, J. *Nature* **1998**, *394*, 337.
- Zhang, B.; Zhang, Y.; Shacter, E.; Zheng, Y. *Biochemistry* **2005**, *44*, 2566.